Materials Research. 2015; 18(4): 806-812
DOI: http://dx.doi.org/10.1590/1516-1439.011815

Formation of Mo−Si−Ti Alloys by Self−propagating Combustion Synthesis

Jie Wu[a], Gaoming Zhu[a], Peizhong Feng[a]*, Xianguo Zhou[a], Xiaohong Wang[a], Farid Akhtar[b]

[a]School of Materials Science and Engineering, China University of Mining and Technology, 221116, Xuzhou, China
[b]Division of Materials Science, Luleå University of Technology, 97187, Luleå, Sweden

Received: May 24, 2015; Revised: July 8, 2015

Test specimens with nominal compositions $MoSi_2$, $(Mo_{0.9}Ti_{0.1})Si_2$, $(Mo_{0.8}Ti_{0.2})Si_2$, $(Mo_{0.7}Ti_{0.3})Si_2$, $(Mo_{0.6}Ti_{0.4})Si_2$, $(Mo_{0.5}Ti_{0.5})Si_2$ and $(Mo_{0.4}Ti_{0.6})Si_2$ were prepared by combustion synthesis. The combustion mode, propagation velocity of combustion wave, combustion temperature and product structure were investigated. Specimens $MoSi_2$, $(Mo_{0.9}Ti_{0.1})Si_2$, $(Mo_{0.8}Ti_{0.2})Si_2$, $(Mo_{0.7}Ti_{0.3})Si_2$, underwent spontaneously self−propagating combustion synthesis. However, the $(Mo_{0.6}Ti_{0.4})Si_2$ and $(Mo_{0.5}Ti_{0.5})Si_2$ specimens required a sustainable energy supply to complete the combustion synthesis reaction. There was no combustion synthesis reaction in specimen $(Mo_{0.4}Ti_{0.6})Si_2$. The combustion wave propagated along a spiral trajectory from top to the bottom of the specimen compacts in a layer by layer mode. The propagation velocity of the combustion wave reduced with the addition of titanium. The X-ray diffraction analysis showed that the Cll_b-$MoSi_2$ and C40-$(Mo,Ti)Si_2$ type phases were formed during combustion synthesis. The intensity of diffraction peaks of C40-$(Mo,Ti)Si_2$ phase increased with Ti content.

Keywords: *intermetallics, silicide, combustion synthesis, self−propagating high−temperature synthesis, X-ray diffraction*

1. Introduction

Molybdenum disilicide is a cheap, non−toxic and environmentally benign intermetallic. It is regarded as a competitive high temperature structural material owing to its high melting point of 2303K, excellent oxidation resistance up to 1873K, moderate density of $6.24 g \cdot cm^{-3}$, low thermal expansion coefficient of 8.1×10^{-6} K^{-1}, good thermal and electrical conductivities of 50 $W \cdot m^{-1} \cdot K^{-1}$ and 21.5×10^{-6} $\Omega \cdot cm$, respectively[1-5]. However, the applications of $MoSi_2$ are limited due to its low fracture toughness at room temperature, poor strength at high temperature and degradation by a phenomenon known as "pesting" (destruction of intermetallic by oxidation into powder) in the temperature range of 673–873 K[5,6]. The key material issues are to improve the fracture toughness and high temperature strength[1-3].

The room temperature fracture toughness and high temperature strength of $MoSi_2$ can be improved by alloying and composite approaches[1-4,7,8]. Alloying promotes the dislocation plasticity in $MoSi_2$ at low temperatures and lowers the brittle−to−ductile transition temperature (BDTT) and results in an increase in room temperature fracture toughness[2-4,7]. The effects of various alloying elements on the ductility of $MoSi_2$ single crystals are reported from first principles calculations[2,9]. The calculations suggest that the alloying addition of Mg, V, Nb, Tc, or Al to the $C11_b$ $MoSi_2$ crystal structure may enhance ductility whereas the addition of Ge, P, or Re is predicted to have an opposite effect[2,9].

Titanium disilicide, $TiSi_2$, has found wide applications as thin film in microelectronics[10-12]. In Ti–Si system, five silicide compounds: Ti_3Si, Ti_5Si_3, Ti_5Si_4, TiSi, and $TiSi_2$ exist[13]. $TiSi_2$ and $MoSi_2$ are of AB_2 type structure with the same atomic percent of silicon. There are $TiSi_2$ and $MoSi_2$ with hexagonal C54 and tetragonal Cll_b structures respectively. The disilicides with C54 and Cll_b crystal structures are closely related by different stacking sequence[14]. The Mo−Si−Ti system can form a ternary compound like $(Mo,Ti)Si_2$[11]. $MoSi_2$ can be toughened by alloying approaches of titanium[15]. So, titanium has great potential as an alloying addition to $MoSi_2$ to improve its performance[15,16].

Several studies have reported that the properties of $MoSi_2$ could be enhanced by alloying with titanium[11,17-19]. Boettinger et al.[16] reported that the $MoSi_2$ composites containing 3mol% and 18mol% $TiSi_2$ have exhibited excellent oxidation resistance at 1300 °C. Yanagihara et al.[17] prepared the specimens with the nominal composition of $(Mo_{0.9}Ti_{0.1})Si_2$ by arc−melting and reported that the pesting of $(Mo_{0.9}Ti_{0.1})Si_2$ was suppressed at temperatures between 673K−973K. $(Mo_{0.9}Ti_{0.1})Si_2$ forms duplex dense and well adherent scale composed of amorphous SiO_2 and rutile at 1500 °C[18].

Combustion synthesis or self−propagating high−temperature synthesis (SHS) provides an attractive alternative to the conventional methods of producing advanced materials, such as ceramics and intermetallics. SHS offers advantages with respect to process economics and process simplicity. The underlying basis of SHS relies on the ability of highly exothermic reactions to be self−sustaining and, therefore, energetically efficient[20-22]. Combustion synthesis is an important method to prepare intermetallics compounds like $MoSi_2$, Ti−Si and Nb−B[23-27]. However, there is no report in the literature on the combustion synthesis of Mo−Si−Ti alloys.

*e-mail: fengroad@163.com

In this study, we have investigated the effect of the alloying of Ti on the combustion synthesis of $MoSi_2$. The combustion synthesis characteristics of the alloys with the nominal composition of $MoSi_2$, $Mo(Si_{0.9}Ti_{0.1})_2$, $Mo(Si_{0.8}Ti_{0.2})_2$, $Mo(Si_{0.7}Ti_{0.3})_2$, $Mo(Si_{0.6}Ti_{0.4})_2$, $Mo(Si_{0.5}Ti_{0.5})_2$, $Mo(Si_{0.4}Ti_{0.6})_2$ are reported. The combustion mode, propagation velocity of combustion wave, combustion temperature and product structure will be discussed.

2. Experimental Procedures

Molybdenum (3−5μm, 99.9% purity), silicon (74μm, 99.5% purity) and titanium (1μm, 99% purity) powders were used as the starting materials. Powder mixtures were prepared with seven different molar ratio including Mo: Si = 1: 2.0 ($0^{\#}$), Mo: Ti: Si = 0.9: 0.1: 2.0 ($1^{\#}$), Mo: Ti: Si = 0.8: 0.2: 2.0 ($2^{\#}$), Mo: Ti: Si = 0.7: 0.3: 2.0 ($3^{\#}$), Mo: Ti: Si = 0.6: 0.4: 2.0 ($4^{\#}$), Mo: Ti: Si = 0.5: 0.5: 2.0 ($5^{\#}$) and Mo: Ti: Si = 0.4: 0.6: 2.0 ($6^{\#}$), corresponding to the nominal composition of $MoSi_2$ ($0^{\#}$), $(Mo_{0.9}Ti_{0.1})Si_2$ ($1^{\#}$), $(Mo_{0.8}Ti_{0.2})Si_2$ ($2^{\#}$), $(Mo_{0.7}Ti_{0.3})Si_2$ ($3^{\#}$), $(Mo_{0.6}Ti_{0.4})Si_2$ ($4^{\#}$), $(Mo_{0.5}Ti_{0.5})Si_2$ ($5^{\#}$) and $(Mo_{0.4}Ti_{0.6})Si_2$ ($6^{\#}$). The powder mixtures were wet mixed in a planetary ball mill for 4 hours using Al_2O_3 balls. Absolute ethanol was used as the milling media. The wet milled slurry was dried and ground and subsequently cold−pressed at an applied pressure of 200MPa into cylindrical compacts; 16mm in diameter and 16mm in height. The relative density of compacts was about 55% of the theoretical.

The combustion synthesis experiments were conducted in a steel combustion chamber with a glass window, under an atmosphere of high purity argon (99.99%, 0.1MPa) (Figure 1). The ignition was accomplished by a heated molybdenum coil with a voltage of 18V and a current of 3A at room temperature.

A color CCD video camera was used to record the combustion synthesis images. The Windows Movie Maker software was applied to analyze the combustion synthesis images and the combustion mode as well as to calculate the propagation velocity of the combustion wave. Thermocouple wires (WRe3−WRe25 with a diameter of 0.1mm) was placed inside a hole drilled in bottom of the powder compacts to record the combustion synthesis temperature with a frequency of 300 Hz. The crystal structure of the combustion products were identified by a Rigaku D/Max−3B X−ray diffractometer (XRD) operating at 35 kV and 30 mA using Cu $K\alpha$ (λ=0.15406 nm) radiation.

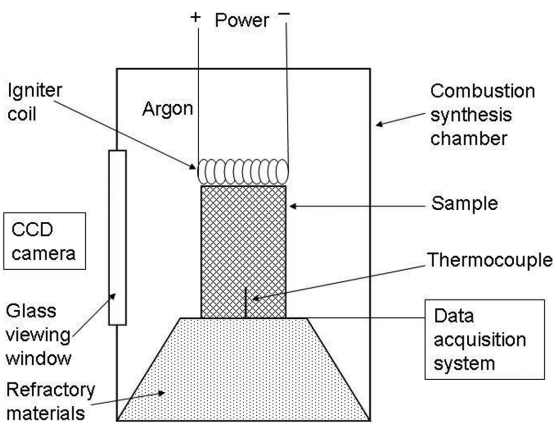

Figure 1. Schematic diagram of experimental combustion synthesis setup.

3. Results and Discussions

3.1. Combustion characteristics

The typical, distinct and representative recorded combustion images (Figure 2) show that the combustion synthesis reaction was ignited locally at the contact point of the specimen with the ignition coil. After ignition, the combustion wave spreaded along a spiral trajectory from top to the bottom of the specimen. This spinning combustion wave is considered as an unstable combustion phenomenon and mainly caused by the lack of sufficient heat flux generated from the reaction to maintain the steady propagation of the planar front[28,29]. We refer it "normal combustion", compared to the explosion combustion; where the propagation velocity of the combustion wave can be up to 1000−4000 m/s[30]. The "normal combustion" refers to the combustion in a combustion chamber of an industrial furnace. The reactants are heated to the ignition temperature by a heater and ignite the combustion reaction locally at the contact point of the reactants with the heater. The local combustion reaction releases sufficient amount of heat to heat up the reactants in the surroundings. This process repeats until all the reactants are consumed. The "normal combustion" phenomenon corresponds to the experimental evidence shown in Figure 2.

The spreading mode of the combustion wave was similar for each specimen, however, the time duration to complete the combustion of the compacts increases with the Ti content. It is necessary to point out that the combustion synthesis reaction of $(Mo_{0.6}Ti_{0.4})Si_2$ and $(Mo_{0.5}Ti_{0.5})Si_2$ specimens was extinguished without a constant heat supply. The $(Mo_{0.4}Ti_{0.6})Si_2$ specimen was not ignited at room temperature, even though some auxiliary measures were adopted, such as preheating[23,28], covering powders between the ignition coil and the green compact[31].

For the formation of compounds, it has been demonstrated empirically that the reaction will not be self−propagating unless the adiabatic temperature is beyond 1800K ($T_{ad} \geq 1800K$)[19-21]. The formula of theoretical adiabatic temperature is as follow[20,29]:

$$-\Delta H^o_{f\,298} = \int_{T_0}^{T_{ad}} C_p \cdot dT \qquad (1)$$

Where, ΔH^o_{298} is the heat of formation of the compound at 298K, T_{ad} is adiabatic temperature of the combustion synthesis reaction, T_o is initial temperature, C_p is the heat capacity.

As shown in Table 1, the theoretical adiabatic temperature of $MoSi_2$ and $TiSi_2$ is 1943K and 1833K, respectively. $MoSi_2$ and $TiSi_2$ satisfy the requirement for self-propagating combustion synthesis theoretically ($T_{ad} \geq 1800K$). Thus $MoSi_2$ and $TiSi_2$ can be formed by combustion synthesis method. The adiabatic temperatures of $(Mo_{1-X},Ti_X)Si_2$ alloys are calculated from the following reaction,

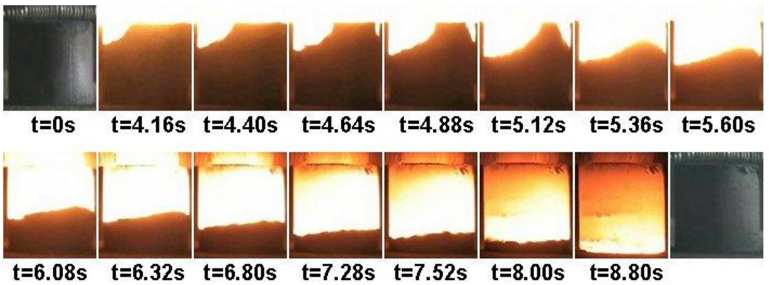

Figure 2. Recorded typical, distinct and representative combustion images of the powder compacts with the nominal composition of $(Mo_{0.7}Ti_{0.3})Si_2$ (3#).

Table 1. The thermodynamics and adiabatic temperature data of $MoSi_2$ and TiSi2.

Alloys	ΔH^{o}_{298} (J ·mol $^{-1}$)	C_p (J ·mol $^{-1}$·K $^{-1}$)	T_{ad}(K)
$MoSi_2$	−131710	$67.831 + 11.970 \times 10^{-3}\ T - 6.569 \times 10^{5}\ T^{-2}$	1943
$TiSi_2$	−134310	$70.417 + 17.573 \times 10^{-3}\ T - 9.037 \times 10^{5}\ T^{-2}$	1833

$$(1-x)Mo + xTi + 2Si \rightarrow (Mo_{1-x},Ti_x)Si_2 \quad (2)$$

In present work, the theoretical adiabatic temperature of seven specimens, including $(Mo_{0.4}Ti_{0.6})Si_2$, are higher than 1800K. Theoretically, $(Mo_{0.4}Ti_{0.6})Si_2$ specimen can undergo combustion synthesis reaction but it did not show combustion synthesis reaction under our experimental conditions. The actual combustion temperature is always lower than the theoretical due to the mass or energy loss in the experiments. The green density of the compacts, furnace atmosphere and the preheating temperature would influence the actual reaction temperature. The alloys with theoretical adiabatic temperature slightly above 1800K, sometimes can not be synthesized by combustion synthesis method at T_o=298K, such as SiC (T_{ad}=1900K), $TaSi_2$ (T_{ad}=1800K)[20,28,32].

3.2. Combustion temperatures

As of the typical combustion temperature–time curve of $MoSi_2$ plot in Figure 3, 298K is the initial temperature, and 1797K is the recorded combustion temperature of $MoSi_2$ compact. This adiabatic temperature is higher than the measured value in our prior experiments[31] and it falls well within the temperature range (1615K−1886K) reported in the literature[23,24]. The recorded temperature is lower than the theoretical adiabatic temperature of 1943K. The difference in recorded and theoretical adiabatic temperature appears to be dependent on the composition of the raw material, reaction environment and heat exchange with the surrounding. Similar experimental evidences are reported earlier in the combustion synthesis of silicide, boride and carbide[25,26,33]. The theoretical adiabatic temperature of Ta_2C, TiSi and NbB_2 are 2600K, 2000K and 2400K, respectively. The measured combustion temperatures reported were 1963K[33], 1603K[25] and 1873K[26], respectively, which are much lower than their theoretical adiabatic temperature.

The combustion temperature−time curves of $(Mo_{0.9}Ti_{0.1})Si_2$(1#), $(Mo_{0.8}Ti_{0.2})Si_2$(2#), $(Mo_{0.7}Ti_{0.3})Si_2$(3#), $(Mo_{0.6}Ti_{0.4})Si_2$(4#) and $(Mo_{0.5}Ti_{0.5})Si_2$(5#) are partially enlarged in Figure 4. Significant differences among these four curves can be

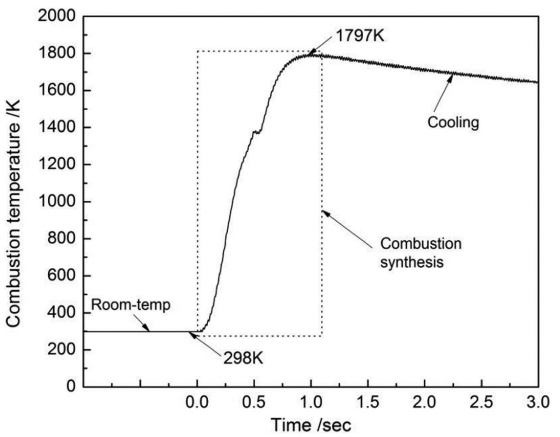

Figure 3. The typical combustion temperature−time curve of $MoSi_2$ specimen.

observed in Figure 4. The combustion synthesis reaction of $(Mo_{0.9}Ti_{0.1})Si_2$, $(Mo_{0.8}Ti_{0.2})Si_2$, $(Mo_{0.7}Ti_{0.3})Si_2$, $(Mo_{0.6}Ti_{0.4})Si_2$ and $(Mo_{0.5}Ti_{0.5})Si_2$ was sustained 0.62s, 0.76s, 0.75s, 0.95s and 1.09s (AB stage) respectively. The time duration of combustion synthesis reaction was prolonged and the combustion front became wider with the increase of Ti content (Figure 4). The rates of temperatures rise at the AB stage (Figure 4) were calculated through the temperature changes at AB stage (the initial temperature is 298 K, the maximum temperatures of 1#-5# are 1650, 1611, 1587, 1743 and 1714 K, respectively) division by the times of the AB stage. The calculated rates of temperatures rise of 1#-5# were 2181, 1728, 1719, 1521 and 1299 K/s, which suggest that the combustion reactions were ultra-fast and combustion rate decreased with the increase of Ti content. The experimental maximum combustion temperatures of $(Mo_{1-x},Ti_x)Si_2$ specimens are shown in Figure 5. At least five iterations were tested for each composition. It shows that the maximum combustion temperature of $MoSi_2$ is the highest

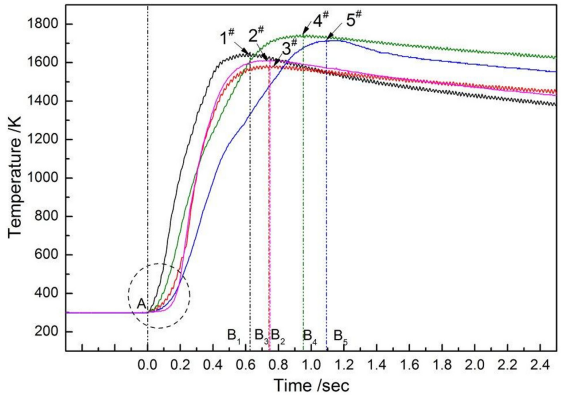

Figure 4. The combustion temperature – time curve for specimen 1#, 2#, 3#, 4# and 5#.

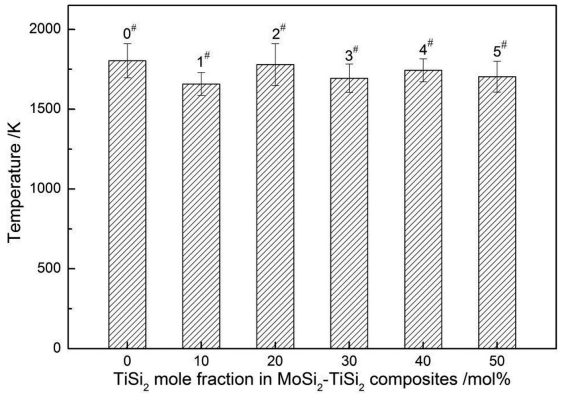

Figure 5. The experimental maximum combustion temperatures of the six different molar ratio samples.

one. But there is no clear trend observed in combustion temperature for other specimens.

3.3. Flame−front propagation velocity

According to the combustion theory, the flame−front propagation velocity of combustion wave is a physical and chemical property of the combustible matter[20]. This is influenced by the chemical composition, diluent content and the density of the compact[20,21]. In present experiments, the specimens are only different in the atomic ratio of Mo−Si−Ti. The flame−front propagation velocity of compacts was deduced from the recorded combustion images. Figure 6 shows the flame−front propagation velocity of the six different specimens. The specimen with the nominal composition of $MoSi_2$ obtains the highest propagation velocity, 3.75 mm/s, and the propagation rate decreases slightly with increasing Ti content, and reaches to a minimum value of 2.50 mm/s at the nominal composition of $(Mo_{0.5}Ti_{0.5})Si_2$. In our case, it is found that the flame−front propagation velocity is significantly influenced by the starting composition.

3.4. X-ray diffraction

The X-ray diffraction (XRD) patterns of the combustion products were shown in Figure 7. It shows that the (Mo,Ti)Si_2 alloys were synthesized by combustion synthesis rapidly.

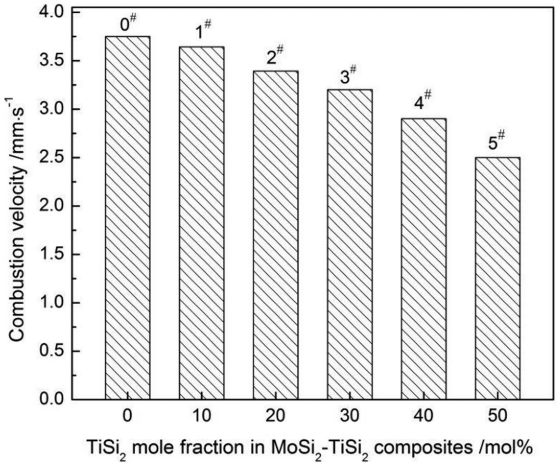

Figure 6. Variation of flame−front velocity of powder compacts with different starting nominal composition.

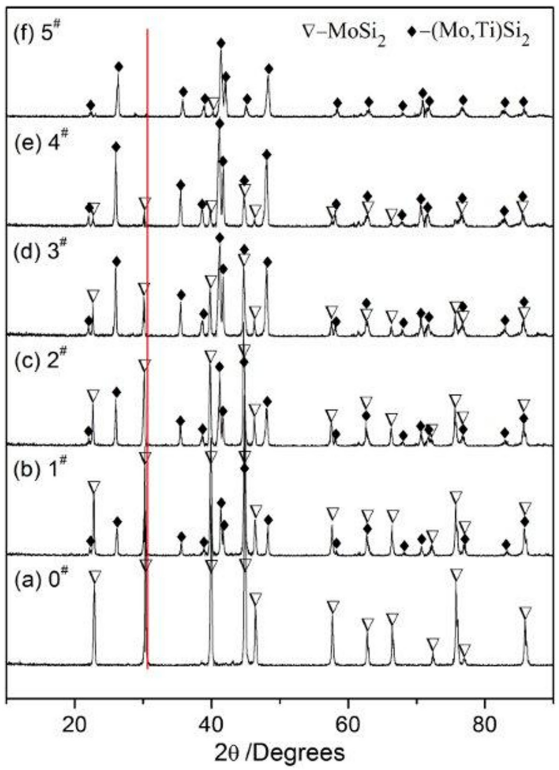

Figure 7. X−ray diffractions patterns of the combustion products with different starting nominal composition.

Figure 7a shows that a Cll_b-type single-phase disilicide, $MoSi_2$, is formed from the specimen 0# with corresponding stoichiometry of Mo: Si = 1: 2.0. Figure 7b indicates that on adding the alloying element of Ti, the diffraction peaks of C40-type phase, (Mo,Ti)Si_2 appear. The nominal composition of $(Mo_{0.9}Ti_{0.1})Si_2$ specimen consists of $Cll_b(MoSi_2)$+ C40((Mo,Ti)Si_2) type phases and it is in agreement with the experimental results of $(Mo_{0.9}Ti_{0.1})Si_2$ prepared by the arc−melting process of Yanagihara et al.[17] Based on the $MoSi_2$-$TiSi_2$ pseudo-binary

diagram, the Cll_b structure has limited solubility of Ti in $MoSi_2$[34]. Svechnikov et al. studied the phase equilibria of Mo−Si−Ti system and found that the structure C40 phase was stabilized by the addition of Ti and extends into the ternary phase region to form the C40 $(Mo,Ti)Si_2$ phase[35]. In current work, dual phase materials with $Cll_b(MoSi_2)$ and C40($(Mo,Ti)Si_2$) were synthesized by in-situ combustion synthesis, this dual phase structure was confirmed by XRD measurement. It is evident that the dual phase structure can be manipulated into other morphologies and size scales[16]. Moreover, the fracture toughness of the dual phase $Cll_b(MoSi_2)$/C40($NbSi_2$) were increased from 1.0–1.4 MPa.$m^{1/2}$ (C40 single phase) to 3.7 MPa.$m^{1/2}$ ($C11_b$/C40 duplex-phase)[36]. With further increase in titanium content (Figure 7), the intensity of the diffraction peaks of Cll_b-$MoSi_2$ phase decreases and increases C40-$(Mo,Ti)Si_2$ phase. It is difficult to identify the XRD peaks of Cll_b-$MoSi_2$ phase in $(Mo_{0.5}Ti_{0.5})Si_2$ specimen, and C40-$(Mo,Ti)Si_2$ is the major phase.

It can be seen from Figure 7a-e, there is a systematic shift of the XRD peaks of $C11_b$−type $MoSi_2$ to lower angles with the increase in the Ti content. It indicates that Ti has made solid solution with $MoSi_2$, and Cll_b−type $(Mo,Ti)Si_2$ is formed. It may be due to the enhanced solid solubility of Ti in $MoSi_2$. Combustion synthesis is a rapid synthesis processing, another non-equilibrium processing technique, that can synthesize supersaturated solid solutions[37]. Therefore, the solid solubility level of Ti in $MoSi_2$ could be enhanced with the increase of the Ti content.

3.5. Microstructure of the products

The scanning electron microscope (SEM) micrographs (Figure 8) of the products show that the microstructure of the samples is uniform and consists of 2-5 μm $(Mo,Ti)Si_2$ particles and uniform arrays of pores. The volume change of samples before and after combustion process is negligible which suggests that the pores between powder particles in the green compacts do not collapse during the combustion synthesis process[38].

Table 2 show the density, crystal structure and lattice parameters of $MoSi_2$ and $(Ti,Mo)Si_2$ phase. The density of $(Mo,Ti)Si_2$ is 4.54 g·cm^{-3}, which is only 72.4% of that of $MoSi_2$. $(Mo,Ti)Si_2$ is an important phase in present experiments, even major phase in $(Mo_{1-X}Ti_X)Si_2$ ($x \geq 0.3$) specimens. Thus, our study opens the way to synthesize light Mo based silicides for high-temperature structural applications.

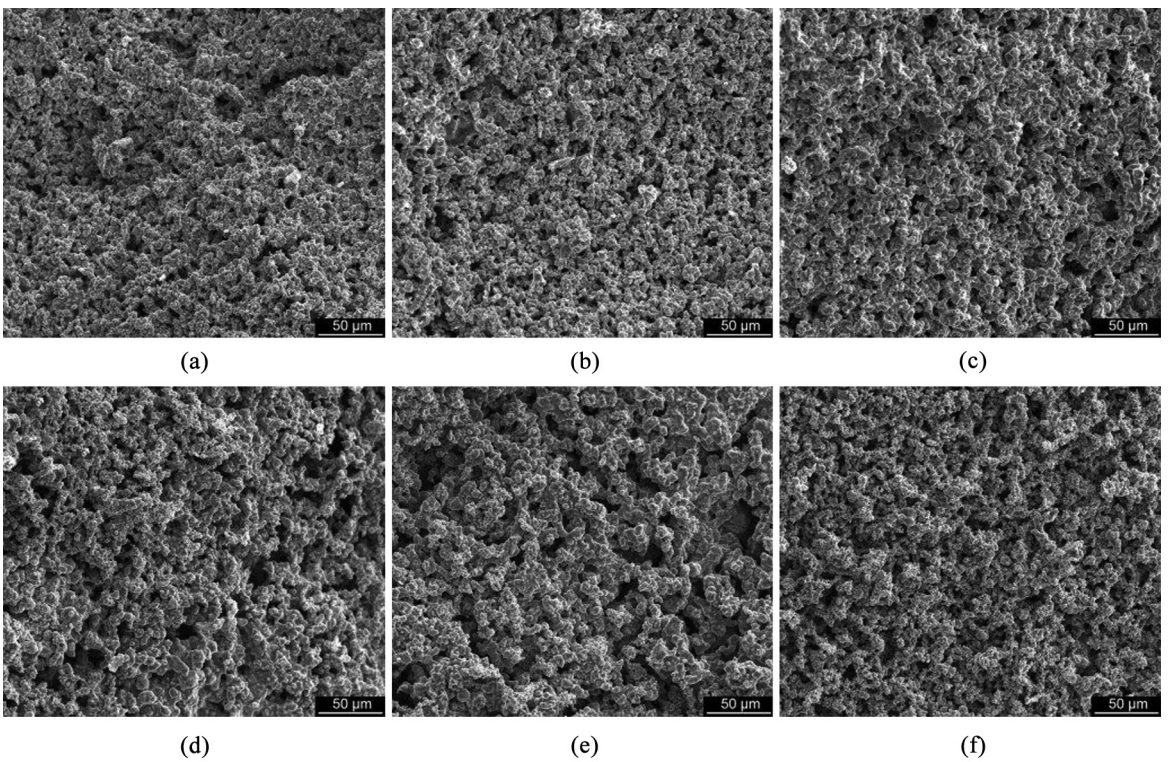

Figure 8. SEM micrographs of the combustion synthesis products, $0^{\#}$ (a), $1^{\#}$ (b), $2^{\#}$ (c), $3^{\#}$ (d), $4^{\#}$ (e) and $5^{\#}$ (f).

Table 2. The density, crystal structure and lattice parameters of $MoSi_2$ and (Mo,Ti)Si2.

Alloys	Density (g·cm^{-3})	Crystal structure	Lattice parameters (nm)			Space Group
			a	b	c	
$MoSi_2$	6.27	Tetragonal	0.3205	-	0.7845	I4/mmm
$(Mo,Ti)Si_2$	4.54	Hexagonal	0.4699	-	0.6524	$P6_222$

4. Conclusions

This study presents an experimental investigation on the combustion synthesis characteristics of $MoSi_2$, $(Mo_{0.9}Ti_{0.1})Si_2$, $(Mo_{0.8}Ti_{0.2})Si_2$, $(Mo_{0.7}Ti_{0.3})Si_2$, $(Mo_{0.6}Ti_{0.4})Si_2$, $(Mo_{0.5}Ti_{0.5})Si_2$ and $(Mo_{0.4}Ti_{0.6})Si_2$ powder compacts. The combustion synthesis reaction was ignited locally at the contact point of compact with the ignition coil, and it quickly spreads to the entire specimen section in a spiral way. It was found that the spinning combustion wave propagated. The flame−front propagation velocity of combustion wave reduced with the increase of the Ti content to $MoSi_2$. The specimens $(Mo_{0.6}Ti_{0.4})Si_2$ and $(Mo_{0.5}Ti_{0.5})Si_2$ needed constant energy supply to keep a self-sustaining reaction. The specimen $(Mo_{0.4}Ti_{0.6})Si_2$ did not ignite at room temperature. The time duration of combustion was prolonged and combustion front was gradually broadened with the Ti content. The crystal structure of products of the specimens with the Ti addition consisted of $Cll_b(MoSi_2)$+ C40($(Mo,Ti)Si_2$) type phases. The XRD peaks of Cll_b phase were gradually weakened, while those of C40 phase were gradually enhanced with the increase of Ti. Alloying with the Ti opens up the way to synthesize light Mo based silicides for high-temperature structural applications.

Acknowledgements

This work was supported by the Fundamental Research Funds for the Central Universities (2013RC18) and National Nature Science Foundation of China (51574241).

References

1. Petrovic JJ and Vasudevan AK. Key developments in high temperature structural silicides. *Materials Science and Engineering*. 1999; A261(1-2):1-5. http://dx.doi.org/10.1016/S0921-5093(98)01043-0.
2. Petrovic JJ. Toughening strategies for MoSi2−based high temperature structural silicides. *Intermetallics*. 2000; 8(9-11):1175-1182. http://dx.doi.org/10.1016/S0966-9795(00)00044-3.
3. Harada Y, Murata Y and Morinaga M. Solid solution softening and hardening in alloyed MoSi2. *Intermetallics*. 1998; 6(6):529-535. http://dx.doi.org/10.1016/S0966-9795(97)00103-9.
4. Zhu GM, Wang XH, Lu Q, Wu GZ and Feng PZ. High-temperature crack-healing behaviour and strength recovery of (MoNb)Si2. *Applied Surface Science*. 2015; 343:41-48. http://dx.doi.org/10.1016/j.apsusc.2015.03.064.
5. Chou TC and Nieh TG. Pesting of the high-temperature intermetallic MoSi2. *JOM*. 1993; 45(12):15-21. http://dx.doi.org/10.1007/BF03222509.
6. Feng P, Wang X, He Y and Qiang Y. Effect of high-temperature preoxidation treatment on the low-temperature oxidation behavior of a MoSi2-based composite at 500 °C. *Journal of Alloys and Compounds*. 2009; 473(1-2):185-189. http://dx.doi.org/10.1016/j.jallcom.2008.06.032.
7. Yi D, Li C, Lai Z, Akselsen OM and Ulvensoen JH. Ternary alloying study of MoSi2. *Metall Mater Trans*. 1998; A29(1):119-129. http://dx.doi.org/10.1007/s11661-998-0164-4.
8. Sharif AA, Misra A, Petrovic JJ and Mitchell TE. Alloying of MoSi2 for improved mechanical properties. *Intermetallics*. 2001; 9(10-11):869-873. http://dx.doi.org/10.1016/S0966-9795(01)00084-X.
9. Waghmare UV, Bulatov V, Kaxiras E and Duesbery MS. Microalloying for ductility in molybdenum disilicide. *Materials Science and Engineering*. 1999; A261(1-2):147-157. http://dx.doi.org/10.1016/S0921-5093(98)01060-0.
10. Murarka SP. Silicide thin film and their applications in microelectronics. *Intermetallics*. 1995; 3(3):173-186. http://dx.doi.org/10.1016/0966-9795(95)98929-3.
11. Gambino JP and Colgan EG. Silicides and ohmic contacts. *Materials Chemistry and Physics*. 1998; 52(2):99-146. http://dx.doi.org/10.1016/S0254-0584(98)80014-X.
12. Chenevier B, Chaix-Pluchery O, Matko I, Madar R and La Via F. Origin of the C49–C54 volume anomaly in TiSi2 thin films: an in−situ XRD and TEM analysis. *Microelectronic Engineering*. 2002; 64(1-4):181-187. http://dx.doi.org/10.1016/S0167-9317(02)00784-0.
13. Massalski TB, Okamoto H, Subramanian PR and Kacprzak L. *Binary alloy phase diagrams*. 2nd ed. Ohio: ASM International Materials Park; 1990.
14. Shah DM, Berczik D, Anton DL and Hecht R. Appraisal of other silicides as structural materials. *Materials Science and Engineering*. 1992; A155(1-2):45-57. http://dx.doi.org/10.1016/0921-5093(92)90311-N.
15. Vasudevan AK and Petrovic JJ. A comparative overview of molybdenum disilicide composites. *Materials Science and Engineering*. 1992; A155(1-2):1-17. http://dx.doi.org/10.1016/0921-5093(92)90308-N.
16. Boettinger WJ, Perepezko JH and Frankwicz PS. Application of ternary phase diagrams to the development of MoSi2−based materials. *Materials Science and Engineering*. 1992; A155(1-2):33-44. http://dx.doi.org/10.1016/0921-5093(92)90310-W.
17. Yanagihara K, Maruyama T and Nagata K. Effect of third elements on the pesting suppression of Mo−Si−X intermetallics (X = Al, Ti, Ta, Zr and Y). *Intermetallics*. 1996; 4:S133-S139. http://dx.doi.org/10.1016/0966-9795(96)00019-2.
18. Yanagihara K, Maruyama T and Nagata K. High temperature oxidation of Mo-Si-X intermetallics (X=Al, Ta, Ti, Zr and Y). *Intermetallics*. 1995; 3(3):243-251. http://dx.doi.org/10.1016/0966-9795(95)98935-2.
19. Nakano T, Nakai Y, Maeda S and Umakoshi Y. Microstructure of duplex−phase NbSi2(C40)/MoSi2(C11b) crystals containing a single set of lamellae. *Acta Materialia*. 2002; 50(7):1781-1795. http://dx.doi.org/10.1016/S1359-6454(02)00030-7.
20. Moore JJ and Feng HJ. Combustion synthesis of advanced materials; Part I. reaction parameters. *Progress in Materials Science*. 1995; 39(4-5):243-273. http://dx.doi.org/10.1016/0079-6425(94)00011-5.
21. Moore JJ and Feng HJ. Combustion synthesis of advanced materials: Part II. classification, applications and modeling. *Progress in Materials Science*. 1995; 39(4-5):275-316. http://dx.doi.org/10.1016/0079-6425(94)00012-3.
22. Merzhanov AG. History and recent developments in SHS. *Ceramics International*. 1995; 21(5):371-379. http://dx.doi.org/10.1016/0272-8842(95)96211-7.
23. Zhang S and Munir ZA. Synthesis of molybdenum silicides by the self−propagating combustion method. *Journal of Materials Science*. 1991; 26(13):3685-3688. http://dx.doi.org/10.1007/BF00557164.
24. Deevi SC. Self−propagating high−temperature synthesis of molybdenum disilicide. *Journal of Materials Science*. 1991; 26(12):3343-3353. http://dx.doi.org/10.1007/BF01124683.

25. Yeh CL, Wang HJ and Chen WH. A comparative study on combustion synthesis of Ti–Si compounds. *Journal of Alloys and Compounds*. 2008; 450(1-2):200-207. http://dx.doi.org/10.1016/j.jallcom.2006.10.074.

26. Yeh CL and Chen WH. Preparation of niobium borides NbB and NbB2 by self−propagating combustion synthesis. *Journal of Alloys and Compounds*. 2006; 420(1-2):111-116. http://dx.doi.org/10.1016/j.jallcom.2005.10.031.

27. Gras C, Gaffet E and Bernard F. Combustion wave structure during the MoSi2 synthesis by mechanically−activated self−propagating high−temperature synthesis (MASHS): In situ time−resolved investigations. *Intermetallics*. 2006; 14(5):521-529. http://dx.doi.org/10.1016/j.intermet.2005.09.001.

28. Yeh CL and Wang HJ. A comparative study on combustion synthesis of Ta−Si compounds. *Intermetallics*. 2007; 15(10):1277-1284. http://dx.doi.org/10.1016/j.intermet.2007.03.004.

29. Merzhanov AG. Solid flames: discoveries, concepts, and horizons of cognition. *Combustion Science and Technology*. 1994; 98(4-6):307-336. http://dx.doi.org/10.1080/00102209408935417.

30. Glassman I. *Combustion*. 3rd ed. New York: Academic Press; 1996.

31. Feng PZ, Liu WS, Islam SH, Wu J, Zhang S, Niu JN et al. Effect of composition of starting materials of Mo–Si on self-propagating high temperature synthesis reaction. *Powder Metall.* 2011; 54(1):79-83. http://dx.doi.org/10.1179/003258910X12678035166818.

32. Yin S. *Combustion synthesis*. Beijing: Metallurgy Industry Press; 1999.

33. Yeh CL and Liu EW. Combustion synthesis of tantalum carbides TaC and Ta2C. *Journal of Alloys and Compounds*. 2006; 415(1-2):66-72. http://dx.doi.org/10.1016/j.jallcom.2005.07.058.

34. Wei FG, Kimura Y and Mishima Y. Microstructure and phase stability in MoSi2–TSi2 (T=Cr, V, Nb, Ta, Ti) pseudo-binary systems. *Materials Transactions*. 2001; 42(7):1349-1355. http://dx.doi.org/10.2320/matertrans.42.1349.

35. Yang Y, Chang YA, Tan L and Du Y. Experimental investigation and thermodynamic descriptions of the Mo-Si-Ti system. *Materials Science and Engineering A*. 2003; 361(1-2):281-293. http://dx.doi.org/10.1016/S0921-5093(03)00560-4.

36. Hagihara K, Maeda S, Nakano T and Umakoshi Y. Indentation fracture behavior of (Mo0.85Nb0.15)Si2 crystals with C40 single-phase and MoSi2(C11b)/NbSi2(C40) duplex-phase with oriented lamellae. *Science and Technology of Advanced Materials*. 2004; 5(1-2):11-17. http://dx.doi.org/10.1016/j.stam.2003.09.007.

37. Suryanarayana C. Mechanical alloying and milling. *Progress in Materials Science*. 2001; 46(1-2):1-184. http://dx.doi.org/10.1016/S0079-6425(99)00010-9.

38. Ran HS, Niu JN, Song BB, Wang XH, Feng PZ, Wang JZ, et al. Microstructure and properties of Ti5Si3-based porous intermetallic compounds fabricated via combustion synthesis. *Journal of Alloys and Compounds*. 2014; 612:337-342. http://dx.doi.org/10.1016/j.jallcom.2014.05.216.